Effect of the divertor geometry on the pedestal confinement in JET-ILW

L. Frassinetti[1], E. Joffrin [2], P. Tamain[2], P. Maget[2] , S. Saarelma[3], J. E. Boom[4], J. Flanagan[3], C. Giroud[3], E. Delabie[5], M. Kempenaars[3,] P. Lomas[3], C. Maggi[3], L. Menes[6] I. Nunes[6] and JET EFDA Contributors*

JET-EFDA, Culham Science Centre, Abingdon, OX14 3DB, UK

[1] Department of Fusion Plasma Physics, Association EURATOM-VR, School of Electrical Engineering, Royal Institute of Technology KTH, SE-10044 Stockholm, Sweden.

[2] CEA, IRFM, F-13108 Saint Paul-lez-Durance, France.

[3]Culham Centre for Fusion Energy, OX14 3DB, Abingdon, United Kingdom

[4]Max-Planck-Institut für Plasma Physik, Boltzmannstr.2, 85748 Garching, Germany

[5] FOM Institute for Plasma Physics Rijnhuizen, Postbus 1207, Nieuwegein, The Netherlands

[6]Centro de Fusao Nuclear, Associacao EURATOM-IST, Lisboa, Portugal

** See the Appendix of F. Romanelli et al., Proceedings of the 24th IAEA Fusion Energy Conference 2012, San Diego, USA*

1. Introduction

The baseline type I ELMy H-mode scenario has been re-established in JET with the new tungsten divertor and beryllium-main wall (JET-ILW) in 2011. In comparison with carbon wall (JET-C) discharges in similar conditions, a degradation of the confinement has been observed, with the reduction mainly driven by a lower pedestal pressure [1]. The causes of the pedestal degradation are not clear yet and are currently under investigations. Some of the main possibilities are a difference in the pedestal stability (possibly driven by the different impurity content between JET-C and JET-ILW) and/or a difference in the recycling flux in the divertor area.

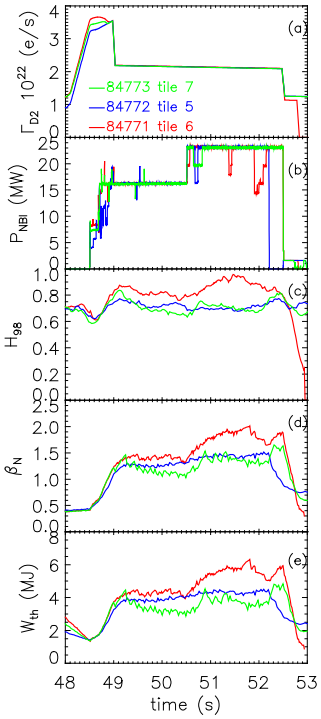

Figure 1. Time traces of gas fuelling (a), NBI power (b), H98 (c), β_N (d) and thermal stored energy (e) for three shots with different outer strike point position.

This work investigates the effect of the magnetic configuration in the divertor region on the pedestal structure, pedestal confinement and ELMs. A set low triangularity H-mode discharges have been performed using the same NBI power (two power levels, 14MW and 22MW) and a similar core shape but changing the strike position relative to the pump throat. Three configurations have been tested: with the outer strike point on the horizontal target (on tile 5), in the corner (tile 6) and on the vertical target (tile 7). Note that this last case has only the outer strike point on the vertical target and it should not be confused with what is typically called vertical

configuration in JET which has both strike points on the vertical target. Most of the discharges have been performed with constant gas fuelling ($\Gamma_{D2}\approx 2\cdot 10^{22}$e/s) but preliminary results from a gas scan are presented as well ($\Gamma_{D2}\approx$1.4-3-5 $\cdot 10^{22}$e/s).

2. Confinement

Figure 1 shows the time evolution of Γ_{D2} , NBI power , H_{98}, β_N and thermal stored energy for three shots with different outer strike point position. The best performance are obtained with the corner configuration (H_{98} up to 0.95 and W_{th} up to 6MJ), while the lowest performance are obtained with the vertical configuration ($H_{98}\approx$0.7 and $W_{th}\approx$4MJ). The result is similar for all the shots analysed, including the power scan and the gas scan. This is shown in figure 2, where the time averaged H_{98} and W_{th} are shown.

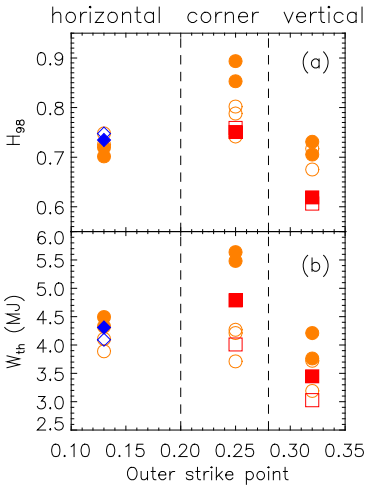

Figure 2. H_{98} (a) and thermal energy (b) vs outer strike position. Red symbols: high Γ_{D2} ($\approx 3.5\cdot 10^{22}$e/s). Orange symbols: medium Γ_{D2}($\approx 2\cdot 10^{22}$e/s). Blue symbols: low Γ_{D2} ($\approx 1.4\cdot 10^{22}$e/s). Open symbols: low power phase. Full symbols: high power phase.

To investigate the origin of the different confinement, the density and temperature profiles in the pre-ELM phase and the effect of the ELMs on the confinement are hereafter studied.

3. Pre-ELM profiles.

The electron density and temperature profiles are studied using the reflectometer and the ECE (when available) and the high resolution Thomson Scattering (HRTS). The ion temperature and the toroidal velocity using the core and edge charge exchange diagnostics. The pre-ELM profiles for the three shots of figure 1 are shown during the high power phase in figure 3. The density, temperature and velocity at the pedestal and in the core are shown for the entire database in figure 4.

From the horizontal to the corner configuration, the major difference is present in the temperature, both for the electron and for the ions: the corner configuration has higher temperature both in the pedestal and in the core. No major difference is observed in the pedestal electron density between the horizontal and the corner configuration while the slightly higher density peaking of the corner configuration (figure 3a) might suggest a difference in the core transport.

From the corner to the vertical configuration, a weak reduction in the temperature (both core and edge) is observed. However, the major difference is present in the electron density: the vertical case has n_e approximately 30% lower than the corner case.

Concerning the toroidal velocity, the plasma with the outer strike point in the corner configuration has the highest rotation, both in the core and at the pedestal.

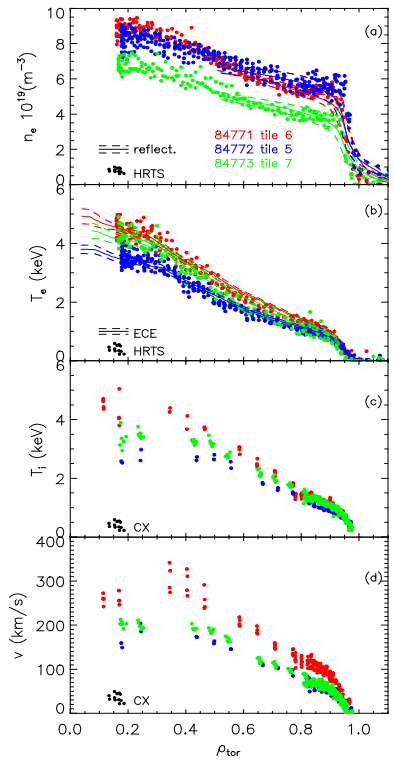

Figure 3. Profiles of electron density (a) electron temperature (b) ion temperature (c) and toroidal velocity (d) in the pre-ELM phase.

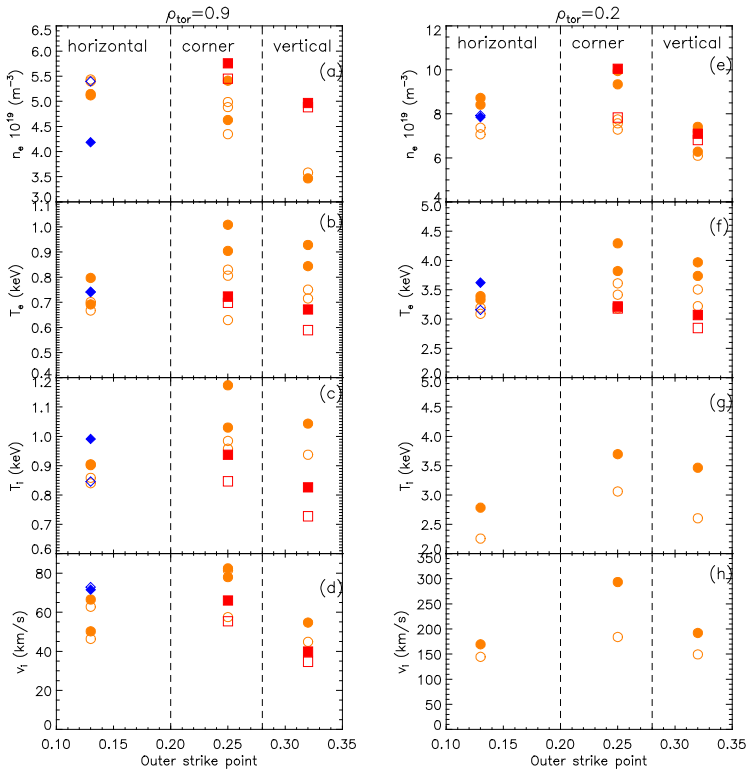

Figure 4. Electron density (first row), electron temperature (second row), ion temperature (third row) and toroidal velocity (third row) at the top of the pedestal at ρ_{tor}=0.9 (left column) and in the core at ρ_{tor}=0.2 (left column).

4. ELM behaviour.

The time evolution of the temperature and density at the pedestal during ELMs is shown in figure 5. In the corner configuration (red lines) the ELMs are very regular and occur with a frequency f_{ELM}=(35±5)Hz and ELM drops $\Delta T_e \approx 250$eV, $\Delta n_e \approx 0.6\ 10^{19} m^{-3}$eV.

The vertical configuration (green lines) has a significantly different ELM behaviour. Phases with high ELM frequency (f_{ELM}≈100Hz) are followed by phases with low frequency (f_{ELM}≈10Hz). During the low frequency phase, the pedestal temperature can reach values comparable to the corner configuration. In this case, the ELM produces a large pedestal temperature drop ΔT_e≈500-600eV while in the low f_{ELM} phase the drops are ≈150eV. The density has a similar behaviour, but values comparable to the corner configuration are not reached.

The pedestal drops of electron temperature and density and the energy losses relative to the pedestal for the entire database are shown in figure 6. The energy losses are calculated for the electron channel only by volume integrating the electron pressure profile before and soon

after the ELMs. It is assumed that the ELM losses for the ions are the same as those of the electrons. The pedestal drops are relatively comparable between the horizontal configuration and the corner configuration. The ELM drops in the vertical configuration are approximately 50% larger.

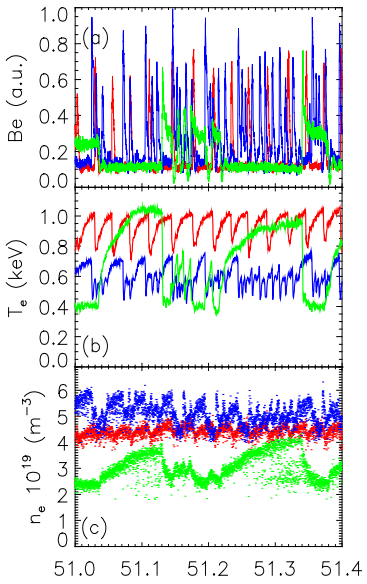

Figure 5. Time traces of Be signal from the outer divertor (a), electron temperature (b) and density (c) for the shots of figure 1 in a 0.4s time interval during the high power phase.

5. Conclusions.

A significant influence on the confinement of the divertor magnetic configuration has been found, despite the unchanged core shape. The highest confinement is observed in the corner configuration and it is due to high pedestal and core density and temperature. The lowest confinement is observed in the vertical configuration and it is due to the low density and to the ELM effect. In fact, the ELMs prevent the vertical configuration to reach a T_e comparable to the horizontal one, as shown in figure 5(b).

The investigation of the recycling effect on the confinement is studied in [2], where a large variation in the particle recycling pattern is observed. However, the 2D transport modelling with EDGE2D and SOLEDGE2D suggests that the observed variations in the recycling are not large enough to explain the change in the confinement.

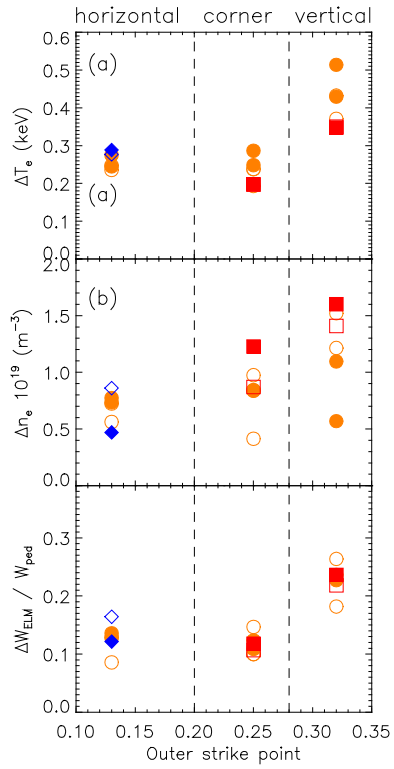

Figure 6. ELM temperature drops (a), density drops (b) and relative ELM energy losses (c).

Acknowledgements

This work was supported by EURATOM and carried out within the framework of the European Fusion Development Agreement. The views and opinions expressed herein do not necessarily reflect those of the European Commission.

References

[1] C. Giroud et al., Nucl. Fusion **53** 113025 (2013)
[2] P. Tamain et al., 21st International Conference on Plasma Surface Interactions (PSI2014), Kanazawa, Japan.